

Ac-Electrogravimetry Study of Electroactive Thin Films. I. Application to Prussian Blue

Claude Gabrielli,^{*,†} Jose J. García-Jareño,^{†,‡} Michel Keddam,[†] Hubert Perrot,[†] and Francisco Vicente[‡]

UPR 15 du CNRS, Physique des Liquides et Electrochimie, Université Pierre et Marie Curie, 4, Place Jussieu, 75252 PARIS CEDEX 05, France, and Department Química-Física, Universidad de Valencia, Dr. Moliner 50, 46100 Burjassot, Valencia, Spain

Received: October 23, 2001

Prussian Blue films were investigated by using ac-electrogravimetry, that is, simultaneous impedance and electrogravimetry spectroscopies at different potentials between the totally reduced form, Everitt's salt, and the mixed-valence compound, Prussian Blue, in KCl solutions. Experimental results allow clear information on the role played by the different ions that are present in the solution to be obtained. It was found that when the film was reduced potassium ions enter the film whereas these are protons that enter at potentials more anodic than the formal potential of the redox process in KCl solutions. It was also proved that potassium ions enter the PB film without water.

Introduction

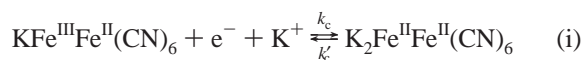
These last years, electroactive thin films were widely investigated and numerous publications are available. Numerous potential technological applications of these materials need the development of thorough studies to understand the relative contribution of the anions and cations to the charge compensation process occurring during the switching of the film between oxidation states. Despite the large quantity of papers, much work still remains to be carried out to understand the electrochemical response of these films. In particular, ingress and release of ions into and from the film can be accompanied by solvent movement either by solvation, exclusion, or other processes.

Ion and solvent transport in electroactive thin films has been investigated by using various methods: first, by recording current and mass changes during potential sweeps by means of an ammeter and a quartz crystal microbalance,^{1–4} second, by measuring the electrochemical impedance of the coated electrode,^{5–8} and then by probe beam deflection (mirage effect).^{9–14} However, these techniques are not sufficiently efficient and selective concerning the separation of the transport of the various species involved in the charge compensation process. Moreover, usually these techniques give information on the global response of the electrode/film/solution interface. As an example, cyclic voltammetry measures the global value of the current, and it is not possible to discriminate between anion ingress or cation expulsion for the charge compensation. In addition, if neutral molecules are involved, their movement is hardly perceptible. Even when cyclic voltammetry was coupled with a quartz crystal microbalance (QCM), which adds the global mass response to the current, their quantitative use is limited to the case where only one species is involved in the charge compensation process. The QCM can be also coupled with other analytical techniques such as radiolabeled techniques; pertinent information was obtained, but the kinetic aspect was rather difficult to explore.¹⁵

Investigation of electroactive films coated on the surface of electrodes has become of special interest in the last years. One of the most studied materials is Prussian Blue (PB), which is $\text{Fe}_4[\text{Fe}(\text{CN})_6]_3$. Prussian Blue is a well-known compound that can be easily deposited on the surface of different types of electrodes.^{16–21} These films present a well-structured crystal building that makes this system very interesting to study the charge transport processes through electroactive films.^{22–26}

Prussian Blue can be obtained in different ways. However, when PB films are galvanostatically produced following the procedure described by Itaya et al.,¹⁸ it is possible to control in a very accurate way the quality and the amount of deposited PB. According to the results of Mortimer and Rosseinsky,^{20,21} the freshly deposited PB films are in the “insoluble” form, $\text{Fe}_4[\text{Fe}(\text{CN})_6]_3$. After several voltammetric cycles in KCl solution, they are converted into the “soluble” structure, which is characterized by the presence of potassium substituting for $1/4$ of the high-spin iron sites in the “insoluble” PB structure ($\text{KFeFe}(\text{CN})_6$).

Prussian Blue films can be reduced to the colorless form, called Everitt's salt ($\text{KFe}_4[\text{Fe}(\text{CN})_6]_3$ or $\text{K}_2\text{FeFe}(\text{CN})_6$, ES), or oxidized to the yellow form called Prussian Yellow ($\text{Fe}_4[\text{Fe}(\text{CN})_6]_3\text{Cl}$ or $\text{KFeFe}(\text{CN})_6\text{Cl}$, PY). These electrochemical processes can be easily detected by cyclic voltammetry of PB films in KCl solution. The reduction process for the “soluble” PB structure has been described as follows:¹⁸



where Fe^{III} and Fe^{II} refer to the different oxidation states of Fe atoms in the PB structure.

The impedance spectra and voltammetric response of PB films in KCl solutions have been the subject of many papers in the past few years.^{22,23,27,28} However, many aspects are not yet clarified about the electrochemical behavior of these films, especially concerning the entry into and exit from the PB film of ions and solvent.

According to the reaction described in scheme i, the reduction of PB to the ES form is accompanied by the entrance of

* To whom correspondence should be addressed. cg@ccr.jussieu.fr.

† Université Pierre et Marie Curie.

‡ Universidad de Valencia.

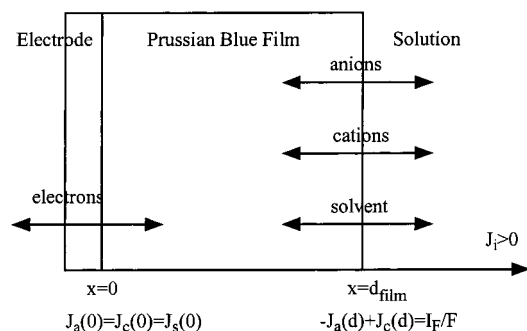


Figure 1. Schema of the electrode/electroactive film/solution system.

potassium ions to maintain the film electroneutrality. However, the insertion or expulsion of ions from the film can also be accompanied by an exchange of solvent molecules between the film and the outer solution.

We propose here to use ac-electrogravimetry, that is, simultaneous coupling of electrochemical impedance and mass/potential transfer function measurements, to characterize ion and solvent motions at the PB film/electrolyte interface. Ac-electrogravimetry allows the mass response to a small potential perturbation to be analyzed thanks to a fast quartz crystal microbalance used in dynamic regime.^{29–31} This technique has been already used for studying oxide materials such as WO_3 ,^{32,33} iron behavior in acidic medium,³⁴ and conducting polymers,^{35–38} and especially polyaniline films.^{39–41}

Theory

In this first approach, charge transfer at the electrode/film interface and mass transport in the solution and in the film are considered as fast as the charge transfer at the film/solution interface, which is considered as the rate-limiting step. This hypothesis is justified for thin films ($\sim 0.1 \mu\text{m}$) and can be controlled by electrochemical impedance measurement. Indeed, when the mass transport process is the rate-limiting step, a Warburg response is observed with a 45° characterizing slope in the electrochemical impedance. If this condition is not fulfilled, theory taking into account limitation by diffusion in the film or migration inside the film was already presented.^{42–45} In this theoretical part, only one cation (solvated or not), one anion, and one free solvent, that is, solvent not in the solvation shell of an ion, are considered for monocharged ions, ($z_i = 1$).

Ion Movement. Figure 1 shows the scheme of the electrode/film/solution. An electrolytic medium was considered from where cation (c), anion (a), and solvent (s) can eventually move through the electrolyte/film interface to neutralize the charges created by the redox reaction of the electroactive film. It should be noted that each ionic species can be accompanied with solvent molecule(s). By definition, the fluxes of species i ($i = c, a, \text{ or } s$), J_i , are positive for outgoing ions:

$$J_i > 0 \quad \text{for } x > 0 \quad i = a, c, s \quad (1)$$

If cations (c), anions (a), and solvent (s) are involved in the redox reaction, the associated mass change and the electric charge passed through the electrode polymer interface, per unit surface, are equal to

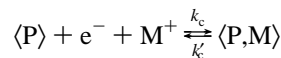
$$\Delta q = -F\Delta\xi_c + F\Delta\xi_a \quad (2)$$

$$\Delta m = m_c\Delta\xi_c + m_a\Delta\xi_a + m_s\Delta\xi_s \quad (3)$$

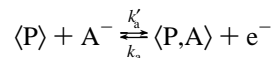
where m_c , m_a , and m_s are the molar masses of the cation (c), the anion (a), and the solvent (s), respectively (if ions are

solvated an extra mass nm_s , where n is the number of solvent molecules is added to their molar mass), and $\Delta\xi_c$, $\Delta\xi_a$, and $\Delta\xi_s$ are the number of moles exchanged for cationic species, anionic species, and solvent per surface unit, respectively.

The doping mechanism of an electroactive film can be described simply by



and



where $\langle P \rangle$ is the host electroactive film and $\langle P, M \rangle$ and $\langle P, A^- \rangle$ are the inserted cation and anion in the electroactive film matrix. Therefore, the net instantaneous molar flux of species i (c, a, or s) is $J_i = d\xi_i/dt$ in $\text{mol cm}^{-2} \text{s}^{-1}$. It can be also expressed in terms of concentration as $C_i = \xi_i/d_{\text{film}}$ where d_{film} is the film thickness. According to the formalism used in another reference and by applying the classical kinetic law for heterogeneous reactions, the time derivative of the concentration C_i is equal for each species to^{46, 40}

$$J_i(d_{\text{film}}) = -\frac{d\xi_i}{dt} = -d_{\text{film}} \frac{dC_i}{dt} = k_i(C_i - C_{i_{\text{min}}}) - k'_i(C_{i_{\text{max}}} - C_i)C_{i_{\text{sol}}} \quad (4)$$

where $dC_i/dt > 0$ for inserted species, $C_{i_{\text{max}}}$ is the maximum concentration of the sites available for insertion, $C_{i_{\text{min}}}$ is the minimum concentration of the sites occupied by the species in the host film, $C_{i_{\text{sol}}}$ is the concentration of species i in the solution, and k_i and k'_i are the kinetic rate constants of transfers, which are potential dependent, $k_i = k_{i0} \exp b_i(E - E_i^0)$ and $k'_i = k_{i0} \exp b'_i(E - E_i^0)$ where E_i^0 is the normal potential.

Steady State and Quasi Steady State. At steady state, the global flux of species is zero, $J_i(x) = 0$; therefore, C_i and E are constants throughout the film. Thus, the derivative of the concentration of the species i with respect to the potential is obtained and is equal to^{39,40}

$$\frac{dC_i(E)}{dE} = \frac{b_i - b'_i}{4} \frac{C_{i_{\text{max}}} - C_{i_{\text{min}}}}{\cosh^2 \left[\frac{(b'_i - b_i)(E - E_i^0 - E_i)}{2} \right]} \quad (5)$$

where E_i was already defined in another paper.⁴⁰

Dynamic Behavior. In the dynamic regime, when a small sine wave potential change, ΔE , is imposed across the metal/film/electrolyte interfaces, low-amplitude sine wave concentrations, ΔC_i , and fluxes, ΔJ_i , are observed such as

$$\Delta J_i(d_{\text{film}}) = -j\omega d_{\text{film}} \Delta C_i = K_i \Delta C_i(d_{\text{film}}) + G_i \Delta E \quad \text{where } i = c, a, s \quad (6)$$

where

$$G_i = [b_i k_i (C_i - C_{i_{\text{min}}}) - b'_i k'_i (C_{i_{\text{max}}} - C_i) C_{i_{\text{sol}}}] \quad (7)$$

and

$$K_i = k_i + k'_i C_{i_{\text{sol}}} \quad (8)$$

where $G_i < 0$ for inserting species and $G_i > 0$ for expelling species.

Then, according to eq 6,

$$\frac{\Delta C_i}{\Delta E}(\omega) = \frac{-G_i}{j\omega d_{\text{film}} + K_i} \quad (9)$$

Thus, the $\Delta C_i/\Delta E(\omega)$ allows the electrochemical impedance, $(\Delta E/\Delta I)(\omega)$, and the electrogravimetric transfer function, $(\Delta m/\Delta E)(\omega)$ to be calculated.

Indeed, the Faradaic current density change, ΔI_F , is related to the charge change, Δq , by $\Delta I_F = j\omega\Delta q$, and by dividing eq 2 and 3 by ΔE and by using eq 6 it comes

$$\frac{\Delta E}{\Delta I}(\omega) = \frac{1}{j\omega C_{\text{interface}} + j\omega d_{\text{film}}F \left[-\frac{\Delta C_c}{\Delta E}(\omega) + \frac{\Delta C_a}{\Delta E}(\omega) \right]} \quad (10)$$

and

$$\frac{\Delta m}{\Delta E}(\omega) = d_{\text{film}} \left[m_c \frac{\Delta C_c}{\Delta E}(\omega) + m_a \frac{\Delta C_a}{\Delta E}(\omega) + m_s \frac{\Delta C_s}{\Delta E}(\omega) \right] \quad (11)$$

where $C_{\text{interface}}$ is the polymer/solution interface capacitance, the electrolyte resistance being neglected here.

By using eq 9, one obtains

$$\frac{\Delta E}{\Delta I}(\omega) = \frac{1}{j\omega C_{\text{interface}} + j\omega d_{\text{film}}F \left[\frac{G_c}{j\omega d_{\text{film}} + K_c} - \frac{G_a}{j\omega d_{\text{film}} + K_a} \right]} \quad (12)$$

and

$$\frac{\Delta m}{\Delta E}(\omega) = -d_{\text{film}} \left(m_c \frac{G_c}{j\omega d_{\text{film}} + K_c} + m_a \frac{G_a}{j\omega d_{\text{film}} + K_a} + m_s \frac{G_s}{j\omega d_{\text{film}} + K_s} \right) \quad (13)$$

Of course, only the charged species, anions and cations, are implied in the electrochemical impedance, $(\Delta E/\Delta I)(\omega)$, whereas the electrogravimetric transfer function, $(\Delta m/\Delta E)(\omega)$, depends on cations, anions, and solvent all together.

Two other interesting quantities can be calculated to discriminate the influence of the various species: the electric charge/potential transfer function, $(\Delta q/\Delta E)(\omega)$, according to eq 10,

$$\frac{\Delta q}{\Delta E}(\omega) = \frac{1}{j\omega} \frac{\Delta I_F}{\Delta E}(\omega) \quad (14)$$

$$= d_{\text{film}}F \left[\frac{G_c}{j\omega d_{\text{film}} + K_c} - \frac{G_a}{j\omega d_{\text{film}} + K_a} \right] \quad (15)$$

and the mass/electric charge-transfer function, $(\Delta m/\Delta q)(\omega)$, where

$$\frac{\Delta m}{\Delta q}(\omega) = j\omega \frac{\Delta E}{\Delta I_F}(\omega) \frac{\Delta m}{\Delta E}(\omega) \quad (16)$$

$$= \frac{-\left(m_c \frac{G_c}{j\omega d_{\text{film}} + K_c} + m_a \frac{G_a}{j\omega d_{\text{film}} + K_a} + m_s \frac{G_s}{j\omega d_{\text{film}} + K_s} \right)}{j\omega F \left[\frac{G_c}{j\omega d_{\text{film}} + K_c} - \frac{G_a}{j\omega d_{\text{film}} + K_a} \right]} \quad (17)$$

It has to be noticed that when only one species, a or c, is involved in the charge exchange, $(\Delta m/\Delta q)(\omega)$ is frequency-independent and equal to m_a/F or m_c/F , respectively.

Partial Electrogravimetric Transfer Functions. Because generally three quantities are unknown, the cation, anion, and solvent responses to ΔE , and only two quantities, $(\Delta E/\Delta I)(\omega)$ and $(\Delta m/\Delta E)(\omega)$ are measured, it is not possible to separately calculate the three unknown quantities. However, it is possible to eliminate the contribution of one species from the mass/potential transfer function. First, the anion (a) response is eliminated from the global electrogravimetric transfer function, $(\Delta m/\Delta E)(\omega)$, by considering^{39,40}

$$\frac{\Delta m_{cs}}{\Delta E}(\omega) = \frac{\Delta m}{\Delta E}(\omega) - \frac{m_a}{F} \frac{\Delta q}{\Delta E}(\omega) \quad (18)$$

By using eq 9 and 11, the partial electrogravimetric transfer function $(\Delta m_{cs}/\Delta E)(\omega)$ relative to cations and solvent alone is equal to

$$\frac{\Delta m_{cs}}{\Delta E}(\omega) = -d_{\text{film}} \left[(m_c + m_a) \frac{G_c}{j\omega d_{\text{film}} + K_c} + m_s \frac{G_s}{j\omega d_{\text{film}} + K_s} \right] \quad (19)$$

In the same way, if a cation contribution is eliminated in the mass change function, the resulting partial electrogravimetric transfer function $(\Delta m_{as}/\Delta E)(\omega)$ is equal to

$$\frac{\Delta m_{as}}{\Delta E}(\omega) = \frac{\Delta m}{\Delta E}(\omega) + \frac{m_c}{F} \frac{\Delta q}{\Delta E}(\omega) \quad (20)$$

and it can be shown that

$$\frac{\Delta m_{as}}{\Delta E}(\omega) = -d_{\text{film}} \left[(m_a + m_c) \frac{G_a}{j\omega d_{\text{film}} + K_a} + m_s \frac{G_s}{j\omega d_{\text{film}} + K_s} \right] \quad (21)$$

From the plot of the partial electrogravimetric transfer functions, the number of species involved in the charge compensation process can be evaluated.⁴¹ This elimination of one species over three is close to the method used by Bruckenstein and Hillman as a diagnostic for species interference.⁴⁷⁻⁴⁹

Example with One Ion. To explain the basic concepts of this approach for simple systems, four main transfer functions, $(\Delta E/\Delta I)(\omega)$, $(\Delta q/\Delta E)(\omega)$, $(\Delta m/\Delta E)(\omega)$, and $(\Delta m/\Delta q)(\omega)$, were calculated from eqs 12, 15, 13, and 17 with one interfering ion, which can be inserted (or expelled) in (or from) the film. Table 1 presents the two typical results for cation and anion exchanges in the case of one involved charged species.

To counterbalance the positive charges created by a potential increasing across the electroactive film, that is, for an oxidation step, the motion of the ionic species is well defined: expulsion of cations or insertion of anions. For this example, the solvent effect is neglected and the molar masses of the ions were given as in KCl solution. The two parameters G_i and K_i were arbitrarily chosen to give reasonable results for the various transfer functions. The four transfer functions $(\Delta E/\Delta I)(\omega)$, $(\Delta q/\Delta E)(\omega)$, $(\Delta m/\Delta E)(\omega)$, and $(\Delta m/\Delta q)(\omega)$ are plotted in Table 1 and parameterized over the frequencies, f , where $\omega = 2\pi f$. The arrows indicate the change of the frequency f from low frequencies to high frequencies. For the electrochemical impedance, $(\Delta E/\Delta I)(\omega)$ (Table 1a and e), the high-frequency loop corresponds to charge transfer in parallel to double-layer charging and the straight line, in the lower frequency range, to ionic transfer. For $(\Delta q/\Delta E)(\omega)$ (Table 1b and f), only one low-frequency loop

TABLE 1: Schematic Representation of the Four Transfer Functions, $(\Delta E/\Delta I)(\omega)$, $(\Delta q/\Delta E)(\omega)$, $(\Delta m/\Delta E)(\omega)$, and $(\Delta m/\Delta q)(\omega)F$

i) Cation expelled	$\frac{\Delta E}{\Delta I}(\omega), \Omega \text{ cm}^2$ (a)	$\frac{\Delta q}{\Delta E}(\omega), \text{C cm}^{-2} \text{ V}^{-1}$ (b)
	Increasing frequencies: \rightarrow	
Values of the parameters:		
$d_{\text{film}} = 0.1 \mu\text{m}$	$\frac{\Delta m}{\Delta E}(\omega), \text{g cm}^{-2} \text{ V}^{-1}$ (c)	$\frac{\Delta m}{\Delta q}(\omega), \text{F, g mol}^{-1}$ (d)
$K_c = 10^{-5} \text{ cm s}^{-1}$		
$m_c = 39 \text{ g mol}^{-1}$		
$G_c = 2 \cdot 10^{-7} \text{ mol cm}^{-2} \text{ s}^{-1} \text{ V}^{-1}$		
$C_{\text{interface}} = 10 \mu\text{F cm}^{-2}$		
ii) Anions inserted	$\frac{\Delta E}{\Delta I}(\omega), \Omega \text{ cm}^2$ (e)	$\frac{\Delta q}{\Delta E}(\omega), \text{C cm}^{-2} \text{ V}^{-1}$ (f)
Values of the parameters:		
$d_{\text{film}} = 0.1 \mu\text{m}$		
$K_a = 10^{-5} \text{ cm s}^{-1}$	$\frac{\Delta m}{\Delta E}(\omega), \text{g cm}^{-2} \text{ V}^{-1}$ (g)	$\frac{\Delta m}{\Delta q}(\omega), \text{F, g mol}^{-1}$ (h)
$m_a = 35 \text{ g mol}^{-1}$		
$G_a = -2 \cdot 10^{-7} \text{ mol cm}^{-2} \text{ s}^{-1} \text{ V}^{-1}$		
$C_{\text{interface}} = 10 \mu\text{F cm}^{-2}$		

is observed, which is related to the charge compensation process, either of the cation or of the anion. These two first electrochemical transfer functions, $(\Delta E/\Delta I)(\omega)$ and $(\Delta q/\Delta E)(\omega)$, do not allow the ionic species to be chemically identified. The electrogravimetric transfer function, $(\Delta m/\Delta E)(\omega)$ (Table 1c and g), is more informative. First, the location of the loop depends on the charge of the ion, this loop is in the third quadrant if cations are expelled and in the first quadrant if anions are inserted. Indeed, according to eq 17, the low-frequency limit of $(\Delta m/\Delta E)(\omega)$ is related to the parameter G_i/K_i . At low frequency, this limit is equal to $(\Delta m/\Delta E)(\omega \rightarrow 0) = -d_{\text{film}}m_iG_i/K_i$, which is a real positive value when ions are inserted as $G_i < 0$ and the loop is located in the first quadrant. On the contrary, when ions are expelled, $G_i > 0$, the sign of $(\Delta m/\Delta E)(\omega \rightarrow 0)$ becomes negative and the semicircle obtained is located in the third quadrant. These results are in good agreement with the electrochemical behavior of the film. Indeed, when this latter is oxidized ($\Delta E > 0$), positive sites are created in the film and if the cation expulsion is the main reaction ($\Delta m < 0$) during the charge compensation, the low-frequency limit of the electrogravimetric transfer function becomes negative ($(\Delta m/\Delta E)(\omega \rightarrow 0) < 0$) as illustrated in Table 1c. If the charge compensation is due to anion insertion, an increase of the mass of the film is induced ($\Delta m > 0$) and, therefore, $(\Delta m/\Delta E)(\omega \rightarrow 0)$ reaches a positive value (Table 1g). Second, the diameter of the $(\Delta m/\Delta E)(\omega)$ depends also on the mass of the involved ionic species, m_i , because $(\Delta m/\Delta E)(\omega \rightarrow 0) = -d_{\text{film}}m_iG_i/K_i$. The last transfer function, $(\Delta m/\Delta q)(\omega)$, gives directly the atomic mass of the ion with a negative value for the cation and a positive value for the anion. Moreover, the ratio mass/charge is independent of the frequencies, f , when only one ionic species is involved in the charge compensation reaction.

Theoretical partial electrogravimetric transfer functions were not plotted in these conditions as according to eq 19 and 21; if

only one ion is taken into account, the theoretical partial electrogravimetric transfer function takes a zero value.

In this paper, Prussian Blue films (PB films) were investigated by ac-electrogravimetry at various potentials to obtain information on the role of the different ions at these potentials. The information extracted from the use of this technique will be analyzed and used to explain several aspects related to the role of protons and potassium ions during the Prussian Blue \leftrightarrow Everitt's salt reaction.

Experimental Section

Film Preparation. FeCl_3 (chemically pure), $\text{K}_3\text{Fe}(\text{CN})_6$, KCl, and HCl (p.a.) (A. R. Merck) were used for the synthesis of PB films. Water was deionized and distilled. One of the Au electrodes on the quartz crystal was immersed into 0.02 M $\text{K}_3(\text{Fe}(\text{CN})_6)$, 0.02 M FeCl_3 , and 0.01 M HCl aqueous solutions. Electrodeposits of PB were galvanostatically carried out by applying a controlled cathodic current of $i_c = 11 \mu\text{A}$ for 210 s.

The film thickness can be estimated from the electro-deposition charge:⁵⁰

$$d_{\text{film}} = \frac{Q}{4FA}(l_0)^3 N_A \quad (22)$$

where Q is the electrodeposition charge (2.31 mC), A is the electrode area (0.27 cm^2), F is the Faraday constant, l_0 is the length of the unit cell (10.17 \AA) of the PB crystal, and N_A is the Avogadro number. The value 4 appears because there are four effective iron atoms per unit cell. The estimated film thickness for these experiments was $d_{\text{film}} = 0.14 \mu\text{m}$.

Experimental Setup. Electrochemical experiments were carried out by means of a typical three electrode cell polarized by using a potentiostat (SOTELEM). PB films were deposited onto one of the gold electrodes of the crystal used as the working electrode, a large area grid made of platinum was used as the counter electrode, and a saturated calomel electrode (SCE) was the reference electrode.

The electrochemical quartz crystal microbalance takes advantage of the change of the resonance frequency of a 6 MHz "AT-cut" quartz crystal (CQE, Troyes, France) due to a minute mass change of one of its electrodes exposed to the solution. The two gold electrodes, deposited on the opposite faces of the quartz crystal, allowed the resonator to be electrically connected to an oscillator circuit. The validity of the Sauerbrey equation⁵¹ was checked with the PB films used in this work through electroacoustic measurements.⁵² In the whole potential range, the microbalance frequency response can be interpreted as a pure mass change if the film thickness is less than $0.15 \mu\text{m}$. Above this limit, film viscoelastic contributions can drastically affect the mass change estimation. An experimental value for the mass/frequency coefficient sensitivity, $-7.5 \times 10^7 \text{ Hz g}^{-1} \text{ cm}^2$, was used for the experimental treatment of all of the gravimetric data; this coefficient was previously estimated through copper electrodeposition.

To use this fast QCM in ac mode, the modified working electrode was polarized at a chosen potential and a sinusoidal small amplitude potential perturbation was superimposed.⁴¹ The microbalance frequency change, $\Delta f_{\text{microbalance}}$, corresponding to the mass response, Δm , of the modified working electrode, was detected by means of a special homemade frequency/voltage converter.⁴¹ The resulting signal was simultaneously sent with the current response, ΔI , of the electrode to a four-channel frequency response analyzer (Solartron 1254), which allowed the electrogravimetric transfer function, $\Delta m/\Delta V(\omega)$, to be simultaneously obtained with the electrochemical impedance,

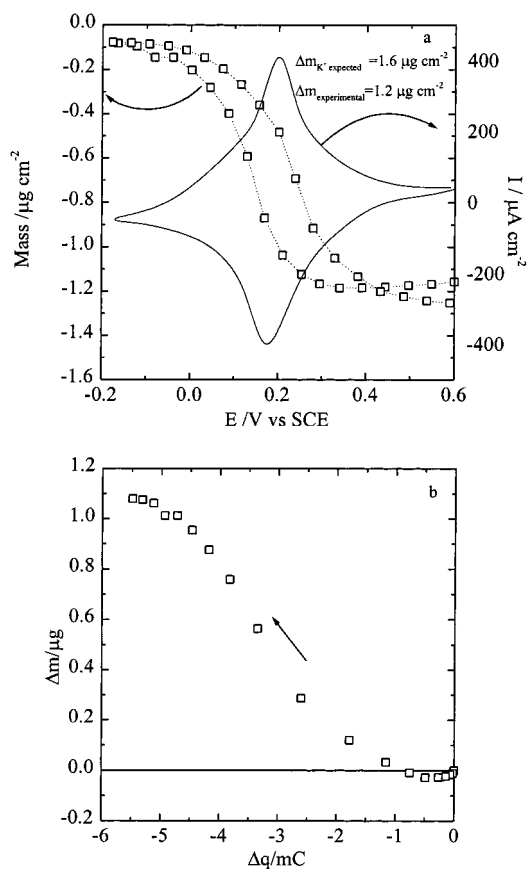


Figure 2. Curve of current-mass vs potential (a) for a PB film in a KCl solution during a linear potential scan (experimental conditions; pH = 2.8, KCl concentration = 0.5 M, scan rate = 20 mV s^{-1} , and reference SCE (potential limits from +0.6 to -0.2 V and from -0.2 to +0.6 V)) and (b) curve mass vs charge for a cathodic sweep (same conditions as previously).

$\Delta V / \Delta I(\omega)$, where ΔV is the raw potential response, which takes into account the electrolyte resistance.

Correction for the Ohmic Drop. To compare experimental results with theoretical ones, the raw electrochemical impedance, $\Delta V / \Delta I(\omega)$, and the raw electrogravimetric transfer function, $\Delta m / \Delta V(\omega)$, were corrected for the ohmic drop in the solution, characterized by the electrolyte resistance, R_{el} , by

$$\frac{\Delta E}{\Delta I}(\omega) = \frac{\Delta V}{\Delta I}(\omega) - R_{\text{el}} \quad (23)$$

and

$$\frac{\Delta m}{\Delta E}(\omega) = \frac{\Delta m}{\Delta V}(\omega) \frac{\frac{\Delta V}{\Delta I}(\omega)}{\frac{\Delta V}{\Delta I}(\omega) - R_{\text{el}}} \quad (24)$$

to be compared with the corresponding quantities calculated from the model presented above.

Results and Discussion

In a first step, current and mass responses to a potential scan were simultaneously measured in KCl aqueous solutions. Then, measurements of the electrochemical impedance and the electrogravimetric transfer function were carried out.

Voltammetric and Mass/Potential Curves. During the reduction of PB films to the colorless Everitt's salt form in KCl solutions, the charge compensation is commonly supposed to

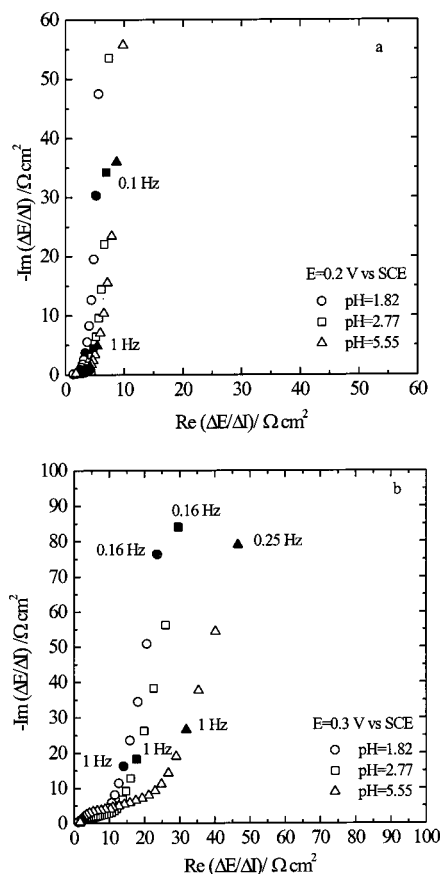


Figure 3. Electrochemical impedance spectra of a PB film at different pH in a KCl 0.5 M solution: (a) $E = +0.2$ V; (b) $E = +0.3$ V. PB film has been cycled for five times at each pH before the EIS measurement takes place to stabilize the system. Changes of the pH values were obtained by additions of HCl.

occur by the entrance of potassium ions within the film.¹⁸ Figure 2a shows a voltammogram of a film of PB in a KCl solution and the change of mass measured through the quartz microbalance accompanying the current variation. The hysteresis observed shows that the electrochemical process is kinetically limited. However, this approach does not allow determination of whether it is mass transport or mass transfer at the film/solution interface that is responsible for kinetic limitations. The mass decrease, Δm , between the reduced (Everitt's salt) and the oxidized (Prussian Blue) form was about $1.2 \mu\text{g cm}^{-2}$. Meanwhile, the expected mass change, Δm , evaluated from the electric charge enclosed within the voltammogram by considering that all of the charge compensation involved only the participation of potassium counterions is about $1.6 \mu\text{g cm}^{-2}$. This discrepancy might show that lighter species were involved in the charge compensation process or that there was a flux of water molecules in the opposite sense to the cation flux or that anions were involved. However, it was not possible to discern between these three possibilities from the global information provided by the quartz microbalance operating in quasi steady state. When the $\Delta m - \Delta q$ curve is plotted (Figure 2b), the calculation of the slope in the linear part gives an equivalent molar mass of 31 g mol^{-1} , which does not correspond to any species present in the solution.

Voltammetric studies of PB films in aqueous KCl solutions showed a Nernstian dependence on the KCl concentration of the redox potential, evaluated from the mean of the anodic and cathodic peak potentials.^{18,19} However, in KCl solution, although the redox potential slightly varied with the pH, the shape of

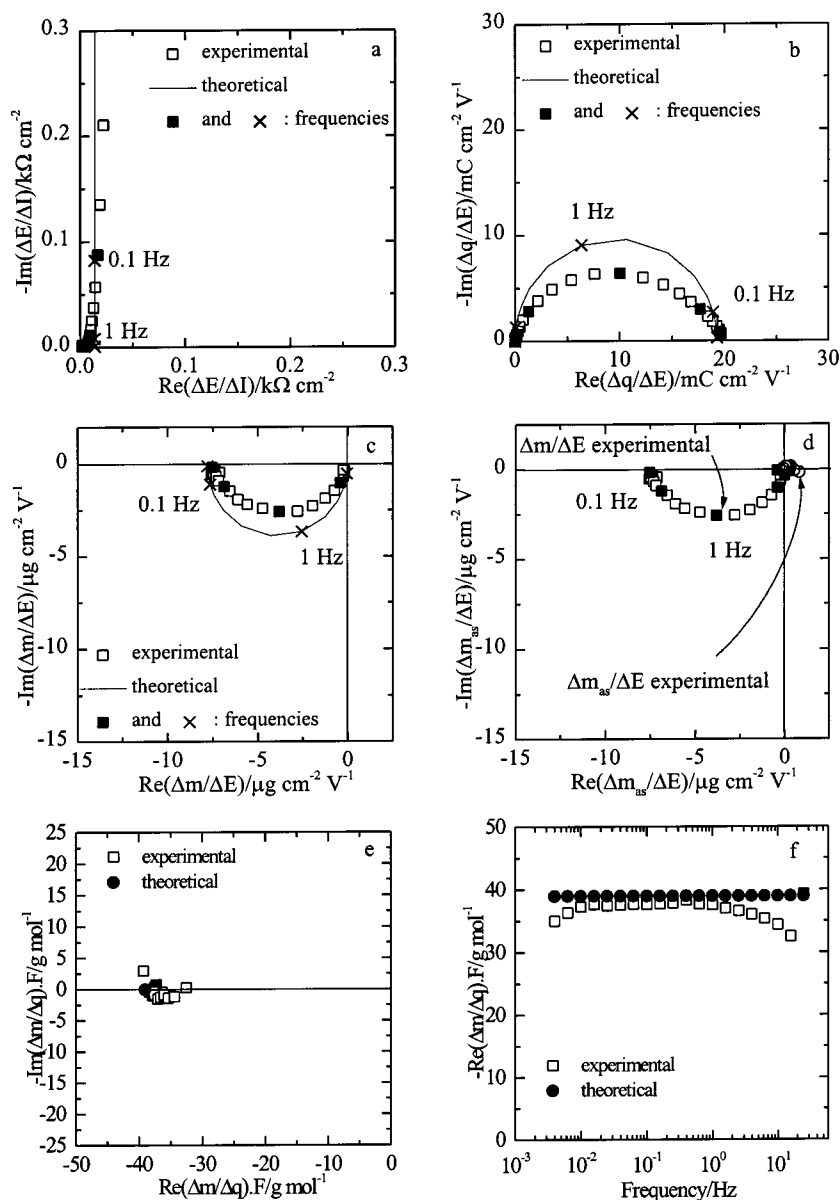


Figure 4. Experimental and theoretical transfer functions at 0.250 V vs SCE in 0.5 M KCl: (a) experimental and theoretical electrochemical impedance, $(\Delta E/\Delta I)(\omega)$, with $d_{\text{film}} = 0.1 \mu\text{m}$, $C_{\text{interface}} = 8 \mu\text{F cm}^{-2}$, $K_c = 4.4 \times 10^{-5} \text{ cm s}^{-1}$, $G_c = 8.8 \times 10^{-7} \text{ mol s}^{-1} \text{ cm}^{-2} \text{ V}^{-1}$; (b) transfer function between the electric charge and the potential, $(\Delta q/\Delta E)(\omega)$, experimental and theoretical data; (c) electrogravimetric transfer function, $(\Delta m/\Delta E)(\omega)$, experimental and theoretical data with $m_c = 39 \text{ g mol}^{-1}$; (d) partial electrogravimetric transfer function, $(\Delta m_{\text{as}}/\Delta E)(\omega)$, with $c = \text{K}^+$; (e) transfer function between the mass and the electric charge, $(\Delta m/\Delta q)(\omega)F$, experimental and theoretical data; (f) real part of the transfer function between the mass and the electric charge, $\text{Re}(\Delta m/\Delta q)F$, as a function of the frequency, experimental and theoretical data.

the voltammograms was shown to be strongly dependent on the pH.⁵³

Electrochemical Impedance Measurements: Influence of the pH. The impedance spectra of the PB film are strongly dependent on the pH of the solution.²⁴ Figure 3 shows the electrochemical impedance spectra for a PB film at various pH at a potential of +0.2 V (Figure 3a), which is the formal potential for the $\text{PB} \rightleftharpoons \text{ES}$ process, and at a potential of 0.3V (Figure 3b). The pH dependence of the electrochemical impedance was much more important at $E = 0.3 \text{ V}$ than at $E = 0.2 \text{ V}$. Because there is no part with a slope equal to 45° in the impedance response (Figure 3a), the rate-limiting step is not mass transport in the film but rather ionic transfer between the solution and the film.

These results indicate, in a qualitative way, that, in addition to the participation of potassium, protons take part in the charge compensation process. This participation changes with the

applied potential during the redox processes, that is, with the oxidation state of the PB film. To quantify the role of each cation (protons and potassium ions) for each potential value and to check whether the solvent or anions can also interfere in the redox process, electrogravimetric transfer function measurements were performed.

Electrogravimetric Transfer Function. The mass response, Δm , of PB films to a small amplitude potential perturbation, ΔE , was studied at several imposed potentials, with respect to the frequency, to obtain extra information about the role of protons and potassium ions during the electrochemical redox reaction of PB. Before carrying out the experiments, one had to wait for the steady state ($I = 0$) to be reached.

Figures 4 and 5 show the four experimental transfer functions for a PB film at two potentials, +0.250 V/SCE and 0.375 V/SCE. Electrochemical impedances, $(\Delta E/\Delta I)(\omega)$, corrected for ohmic drop according to eq 23, are shown in Figures 4a and

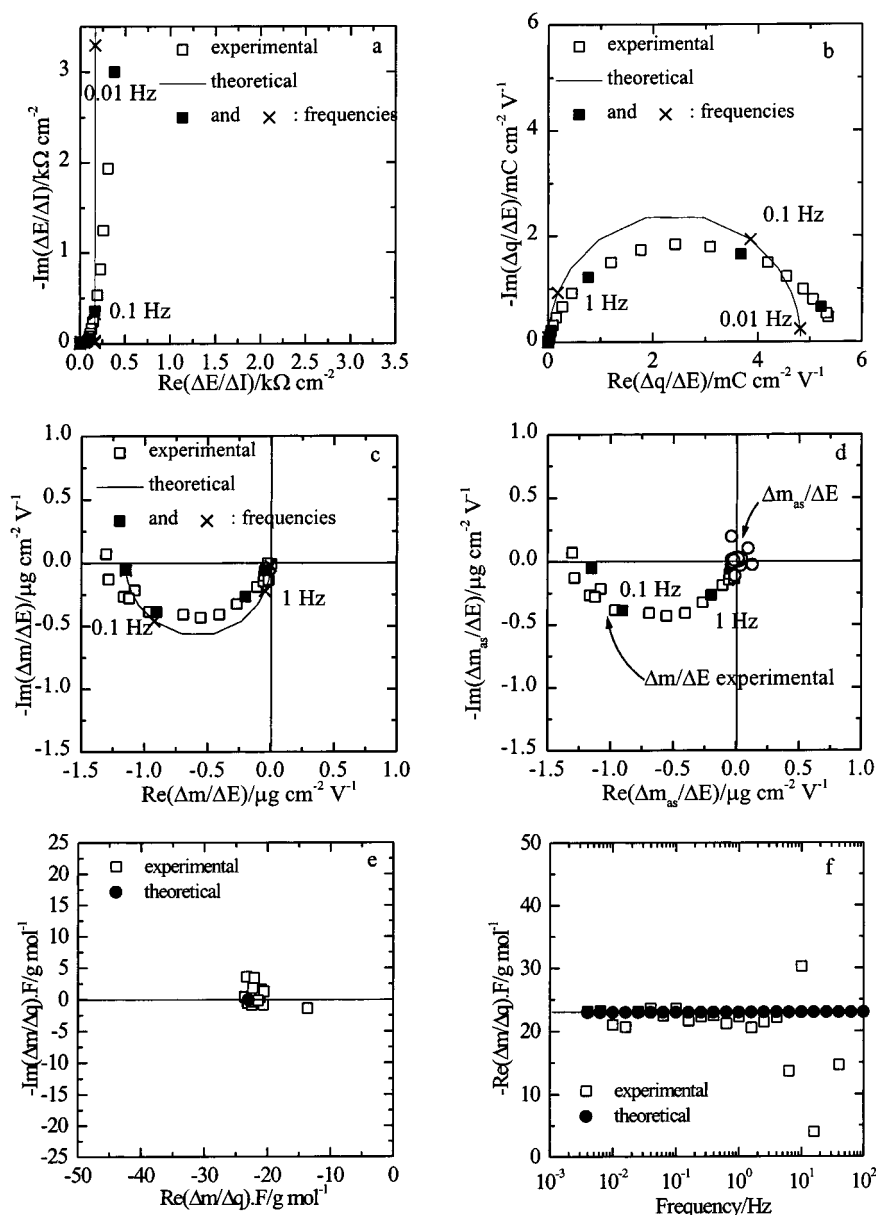


Figure 5. Experimental and theoretical transfer functions at 0.375 V vs SCE in 0.5 M KCl: (a) experimental and theoretical electrochemical impedance, $(\Delta E/\Delta I)(\omega)$, with $d_{\text{film}} = 0.1 \mu\text{m}$, $C_{\text{interface}} = 8 \mu\text{F cm}^{-2}$, $K_c = 1.2 \times 10^{-5} \text{ cm s}^{-1}$, $G_c = 6.3 \times 10^{-8} \text{ mol s}^{-1} \text{ cm}^{-2} \text{ V}^{-1}$; (b) transfer function between the electric charge and the potential, $(\Delta q/\Delta E)(\omega)$, experimental and theoretical data; (c) electrogravimetric transfer function, $(\Delta m/\Delta E)(\omega)$, experimental and theoretical data with $m_c = 23 \text{ g mol}^{-1}$; (d) partial electrogravimetric transfer function, $(\Delta m_{\text{as}}/\Delta E)(\omega)$ with $m_c = 23 \text{ g mol}^{-1}$; (e) transfer function between the mass and the electric charge, $(\Delta m/\Delta q)(\omega)F$, experimental and theoretical data; (f) real part of the transfer function between the mass and the electric charge, $\text{Re}(\Delta m/\Delta q)F$, as a function of the frequency, experimental and theoretical data.

5a. Then, $(\Delta q/\Delta E)(\omega)$ were calculated by using $(\Delta E/\Delta I)(\omega)$ experimental data and plotted in Figures 4b and 5b. A single loop was obtained for the two potentials. This means that only one type of species, anions or cations, was involved in the redox reaction, but the charge of the ion was not determined as it was previously indicated in Table 1b and f. Moreover, the role of the solvent was not clarified at this stage. The experimental electrogravimetric transfer function, $(\Delta m/\Delta E)(\omega)$, experimentally corrected for ohmic drop (eq 24), is presented in Figures 4c and 5c. Only one semicircle is obtained, and its location in the third quadrant indicates that the ionic species involved here was a cation (Table 1c). This single loop confirms the lack of a contribution of anions for this material. As the relaxation times are usually different for anions, cations, and free solvent (see companion paper), if only one loop is observed, it means that only one species is involved in the redox process. If two ionic species have the same charge, only one loop is found whatever

their molar mass. But, the chemical identification of the species is not available at this step. Only, the partial electrogravimetric transfer function allows an identification of the ions. From eq 20, $(\Delta m_{\text{as}}/\Delta E)(\omega)$ was experimentally calculated and presented in Figures 4d and 5d. Figure 4d corresponds to the elimination of the potassium ion contribution ($E = 0.250 \text{ V}$, $m_c = 39 \text{ g mol}^{-1}$) and Figure 5d to the elimination of the hydronium contribution ($E = 0.375 \text{ V}$, $m_c = 19 \text{ g mol}^{-1}$). In both cases, these partial electrogravimetric functions, $(\Delta m_{\text{as}}/\Delta E)(\omega)$, are very small showing that it is mainly K^+ that is involved in the charge compensation process at 0.250 V and H_3O^+ at 0.375 V. This result implies that, according to the theory, the contribution of anions and water molecules are always negligible in this potential range. In addition, the contribution of the potassium ions was negligible at $E = 0.375 \text{ V}$, while for a potential of $E = 0.250 \text{ V}$, it is the contribution of hydrated protons that was less important.

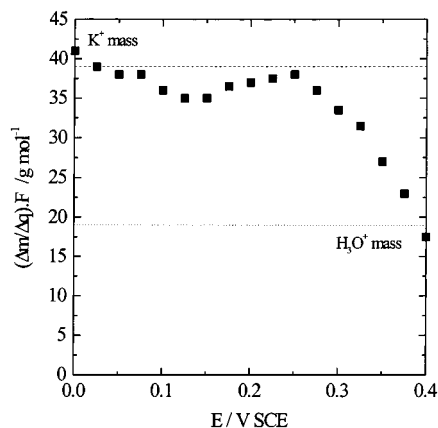


Figure 6. Dependence of the low-frequency limit of the $(\Delta m/\Delta q)(\omega)$ function on the potential. Experimental conditions were pH = 2.2, [KCl] = 0.5 M.

At last, $(\Delta m/\Delta q)(\omega)$ was experimentally calculated according to eq 16. This transfer function is an attractive parameter to identify the nature of the ion that was involved in the charge compensation process, especially when only one cation acts as counterion. Note that $(\Delta m/\Delta q)(\omega)$ is defined to be negative when cations act as counterions (Table 1d) and positive for anion participation (Table 1b). Therefore, when only one species is involved in the compensation process, $(\Delta m/\Delta q)(\omega)F$ is frequency-independent and directly gives its molar mass as it is plotted in Figures 4e and 5e. At $E = 0.250$ V/SCE, $(\Delta m/\Delta q)(\omega)F$ is equal to -39 g mol $^{-1}$; otherwise at $E = 0.375$ V/SCE, $(\Delta m/\Delta q)(\omega)F$ is around -23 g mol $^{-1}$. At a potential of $E = 0.375$ V/SCE, the absolute values obtained for this parameter are between 20 and 25 g mol $^{-1}$ in a wide range of frequencies (Figure 4f). This value, not so far from the solvated proton mass, 19 g mol $^{-1}$, indicates that at this potential it is mainly the hydronium ion that participates in the charge compensation process as a counterion. On the other hand, at a potential of $E = 0.250$ V/SCE, the $(\Delta m/\Delta q)(\omega)F$ quantity had values of about 39 g mol $^{-1}$, also in a wide range of frequencies (Figure 5f), which are close to the 38.9 g mol $^{-1}$ corresponding to the potassium atomic mass. It is important to note that the $(\Delta m/\Delta q)(\omega)F$ is not dependent on the frequency. If this function varies with frequency that means that faster and slower processes take place by the incorporation–expulsion of different species. For the higher frequencies, the $\Delta m/\Delta E$ limit is zero. This means that no species is transferred faster than the experimental time scale. In the PB film case, at both potentials, it is proved that mainly two species participate in the charge compensation process. Therefore, at a potential equal to 0.2 V, it is the nonhydrated potassium ions that played the role of counterion. This result agrees with those by Zadroncki et al.,⁵⁴ which have shown that potassium and ammonium cations enter dehydrated within the PB film during the reduction process. For the two potentials, the four main transfer functions, $(\Delta E/\Delta I)(\omega)$, $(\Delta q/\Delta E)(\omega)$, $(\Delta m/\Delta E)(\omega)$, and $(\Delta m/\Delta q)(\omega)$, were calculated from eq 12, 15, 13, and 17 and compared with experimental results. In all cases, the theoretical plots were in good agreement in terms of shape and frequency distributions. Moreover, the basic parameters, m_c , K_c , and G_c , chosen for the calculations were the same for the four transfer functions, which validates the proposed model.

Figure 6 shows the dependence of the low-frequencies limit of $(\Delta m/\Delta q)(\omega)F$, which gives an apparent molar mass, m_c , of the cations expelled from Prussian Blue, with respect to the potential. It is observed that in a wide range of potentials, between 0 and 0.25 V, this function reaches values near the

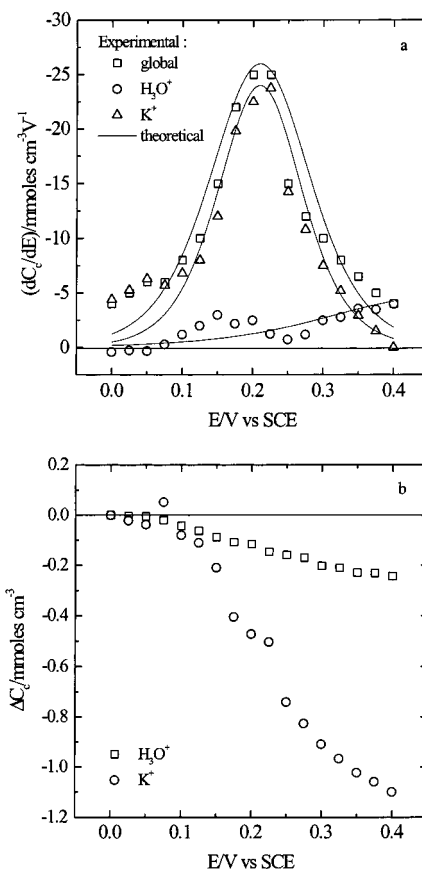


Figure 7. Variation of the derivative of the insertion law (a) for K^+ and H_3O^+ ions with the potential $(dC_c(E)/dE)$ (experimental conditions; pH = 2.2, [KCl] = 0.5 M). Theoretical values were taken in cgs units, and to simplify the calculations, β , γ , and η are defined as follows: $\beta = ((b_i - b'_i)/4)(C_{i,max} - C_{i,min})$; $\gamma = (b'_i - b_i)/2$; $\eta = -((b'_i - b_i)/2)(E_i^0 - E_i)$; for global, $\beta = -0.026$, $\gamma = 10.5$, and $\eta = -2.2$; for H_3O^+ , $\beta = -0.0045$, $\gamma = 5$, and $\eta = -2.2$; for K^+ , $\beta = -0.024$, $\gamma = 12.5$, and $\eta = -2.6$. Panel b shows the variation of the insertion law for K^+ and H_3O^+ ions with the potential $(\Delta C_c(E))$ with the same experimental conditions as for panel a.

potassium molar mass. Otherwise, at potentials more anodic than 0.35 V, the obtained molar mass approximated the mass of hydrated proton. This result explains the smaller values of apparent molar mass already found in the literature.⁵⁴ Between these two potentials, intermediate values of molar mass were obtained. This shows that the two cations are simultaneously involved in the charge compensation process.

From these results, it was concluded that the only contributions to the $(\Delta m/\Delta E)(\omega)$ function that have to be considered for this system were those of the potassium and proton ions, and therefore, the partial contribution of both cations can be evaluated from eqs 10 and 11.

Figure 7a shows the plot of the quantity $-G_c/K_c$, which is equal, from eq 9, to $(\Delta C_c/\Delta E)(0)$, that is, the derivative of the insertion law (eq 5), with respect to the potential. The contribution of both ions at different potentials, also plotted in Figure 7a, is obtained by taking into account the relative proportion of these ions in the compensation process known from the apparent molar mass shown in Figure 6. It is observed that the role of hydrated protons is especially important at potentials between $E = 0.3$ V and $E = 0.4$ V, where the film is in the Prussian Blue form. At potentials more cathodic than 0.3 V, the hydronium contribution became negligible if compared with the potassium contribution. This confirms that the charge compensation process during reduction mainly took place by incorpora-

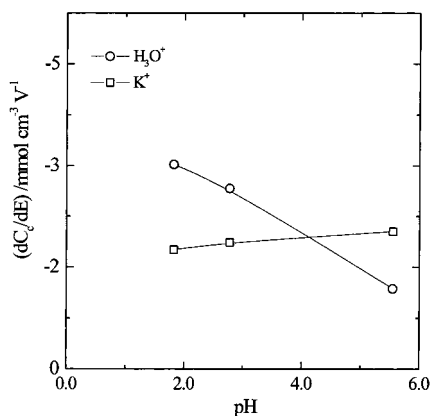


Figure 8. Variation of the derivative of the insertion law for K^+ and H_3O^+ ions with the pH. Experimental conditions were $E = +0.375$ V vs SCE and $[KCl] = 0.5$ M.

tion of potassium ions. Figure 7b shows the isotherm laws for both ions obtained by integration of Figure 7a. This allows the quantities $C_{c_{max}} - C_{c_{min}}$ to be estimated. It should be noted that both potassium and proton insertion takes place when PB films are reduced from the PB form to the ES form. However, the involved quantity of H_3O^+ ions is six times lower than the quantity of K^+ ions when PB is switched between oxidized states.

These results help to explain the pH dependence of the electrochemical impedance, although the redox potential of the $PB \leftrightarrow ES$ process mainly depends on the KCl concentration. In fact, it is observed that the contribution of the K^+ is very much larger than the contribution of the hydrated proton in a wide range of potentials, which agrees with the reaction of the scheme i. However, it has been proposed that the hydrated protons participate in the conduction mechanism through the film.^{24,53} This electronic conduction through the film has been described as an electron-hopping process where the hydrated proton ions must be fixed on the appropriate site to allow the electron transfer between two neighboring iron sites in the PB crystal structure. Then, at potentials between 0.3 and 0.4 V, a protonation (H_3O^+ insertion) of the film takes place. For lower potentials, the oxidation or reduction processes occur by the participation of potassium ions.

Figure 8 shows the influence of pH on the derivative of the insertion/expulsion isotherm. It confirms that K^+ insertion/expulsion is practically pH-independent whereas the H_3O^+ insertion/expulsion rate decreases when pH increases, that is, when H^+ concentration decreases in the bathing solution.

Finally, a remark can be made concerning the adequateness of the model with the experimental results. As shown in Figures 3 and 4, the calculated quantities from the model have semicircular shapes, whereas the experimental results show depressed semicircular loops. This is a very common feature of the electrochemical impedances measured on solid electrodes. This discrepancy is phenomenologically explained in that field by using a constant phase element (CPE) in the equivalent circuit instead of a first-order time constant:

$$\frac{\Delta C_c(\omega)}{\Delta E} = \frac{-G_c}{(j\omega)^{\alpha_c} d_{\text{film}} + K_c}$$

instead of $\frac{\Delta C_c(\omega)}{\Delta E} = \frac{-G_c}{j\omega d_{\text{film}} + K_c}$

Figure 9 shows an example of the calculated quantity $(\Delta m/\Delta E)(\omega)$ taking into account a constant phase element (CPE)

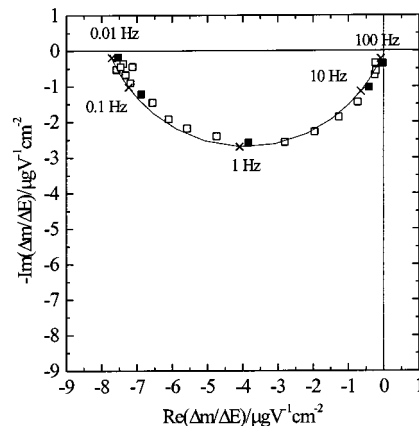


Figure 9. Experimental and theoretical electrogravimetric transfer function at 0.250 V vs SCE with α_c parameter ($\alpha_c = 0.85$ and same values for the other parameters as in Figure 4).

with $\alpha_c = 0.85$. When this assumption is considered, the model predicts a mass/potential transfer function very close to the corresponding experimental data. The kinetic parameters used to calculate this quantity are not very different from the quantities obtained without taking into account a CPE in the model.

Concerning the impedance, a CPE is generally due to nonuniformity at the electrode surface; for mass measurements, similar causes can be evoked. First of all, even if the quartz microbalance has a radial dependence of the mass sensitivity, this should not affect the frequency dependence of the mass/potential transfer function. On the contrary, if the thickness of the polymer layer is not uniform, such a behavior can be observed. Some distribution of the thickness of the polymer film has already been shown to affect the impedance of the modified electrode by a polymer.^{55,56}

Conclusion

The ac-electrogravimetric measurements on PB films at different potentials give valuable information on the chemical nature and the amount of ions that can enter or leave the PB film at a given potential, whereas the information provided by the mass changes measurement by means of a quartz crystal microbalance in quasi steady state during a voltammetric scan is only global.

It is possible to discern between the role of hydrated protons and potassium ions by means of ac-electrogravimetry. At potentials where the film is in the mixed-valence form (PB form), the hydrated proton plays a very important role while potassium ions do not act as counteraction. At potentials more cathodic, the contribution of protons is almost negligible compared with the contribution of potassium ions.

References and Notes

- (1) Bruckenstein, S.; Hillman, A. R. *J. Phys. Chem.* **1988**, *92*, 4837.
- (2) Orata, D.; Buttry, D. A. *J. Am. Chem. Soc.* **1987**, *109*, 3574.
- (3) Torresi, R. M.; Cordoba-Torresi, S. I.; Gabrielli, C.; Keddad, M.; Takenouti, H. *Synth. Met.* **1993**, *61*, 291.
- (4) Naoi, K.; Lien, M.; Smyrl, W. H. *J. Electrochem. Soc.* **1991**, *138*, 440.
- (5) Maiari, G.; Torresi, R. M.; Ticianelli, E. A.; Nart, F. C. *J. Phys. Chem.* **1996**, *100*, 15910.
- (6) Deslouis, C.; Musiani, M.; Tribollet, B. *J. Phys. Chem.* **1996**, *100*, 8994.
- (7) Deslouis, C.; Musiani, M.; Tribollet, B.; Vorotyntsev, M. A. *J. Electrochem. Soc.* **1995**, *142*, 1902.
- (8) Glarum, S. H.; Marshall, J. H. *J. Electrochem. Soc.* **1987**, *134*, 142.
- (9) Mathias, M. F.; Haas, O. J. *J. Phys. Chem.* **1992**, *96*, 3174.
- (10) Matencio, T.; Vieil, E. *Synth. Met.* **1991**, *44*, 349.

- (11) El Rhazi, M.; Lopez, C.; Deslouis, C.; Musiani, M. M.; Tribollet, B.; Vieil, E. *Synth. Met.* **1996**, *78*, 59.
- (12) Barbero, C.; Miras, M. C.; Kotz, R.; Haas, O. *J. Electroanal. Chem.* **1997**, *437*, 191.
- (13) Henderson, M. J.; Hillman, A. R.; Vieil, E. *J. Phys. Chem. B* **1999**, *103*, 8899.
- (14) Henderson, M. J.; Hillman, A. R.; Vieil, E. *J. Electroanal. Chem.* **1998**, *454*, 1.
- (15) Malik, M. A.; Horanyi, G.; Kulesza, P. J.; Inzelt, G.; Kertesz, V.; Schmidt, R.; Czirok, E. *J. Electroanal. Chem.* **1998**, *452*, 57.
- (16) Neff, V. D. *J. Electrochem. Soc.* **1978**, *125*, 886.
- (17) Itaya, K.; Shibayama, K.; Akahoshi, H.; Toshima, S. *J. Appl. Phys.* **1982**, *53*, 804.
- (18) Itaya, K.; Ataka, T.; Toshima, S. *J. Am. Chem. Soc.* **1982**, *104*, 4767.
- (19) Itaya, K.; Akahoshi, H.; Toshima, S. *J. Electrochem. Soc.* **1982**, *129*, 1498.
- (20) Mortimer, R. J.; Rosseinsky, D. R. *J. Electroanal. Chem.* **1983**, *151*, 133.
- (21) Mortimer, R. J.; Rosseinsky, D. R. *J. Chem. Soc., Dalton Trans.* **1984**, 2059.
- (22) Feldman, B. J.; Melroy, O. *J. Electroanal. Chem.* **1987**, *234*, 213.
- (23) Feldman, B. J.; Murray, R. W. *Inorg. Chem.* **1987**, *26*, 1702.
- (24) García-Jareño, J. J.; Navarro-Laboulais, J.; Vicente, F. *Electrochim. Acta* **1996**, *41*, 835.
- (25) Piela, P.; Wrona, P. K.; Galus, Z. *J. Electroanal. Chem.* **1994**, *378*, 159.
- (26) Inove, H.; Yanagisawa, S. *J. Inorg. Nucl. Chem.* **1974**, *36*, 1409.
- (27) García-Jareño, J. J.; Navarro, J.; Roig, A. F.; Scholl, H.; Vicente, F. *Electrochim. Acta* **1995**, *40*, 1113.
- (28) Kulesza, P. J. *J. Electroanal. Chem.* **1990**, *289*, 103.
- (29) Cordoba-Torresi, S.; Gabrielli, C.; Keddám, M.; Takenouti, H.; Torresi, R. *J. Electroanal. Chem.* **1990**, *290*, 261.
- (30) Bourkane, S.; Gabrielli, C.; Keddám, M. *Electrochim. Acta* **1989**, *34*, 1081.
- (31) Bourkane, S.; Gabrielli, C.; Huet, F.; Keddám, M. *Electrochim. Acta* **1993**, *38*, 1023, 1827.
- (32) Gabrielli, C.; Keddám, M.; Perrot, H.; Torresi, R. *J. Electroanal. Chem.* **1994**, *378*, 85.
- (33) Bohnke, O.; Vuillemin, B.; Gabrielli, C.; Keddám, M.; Perrot, H.; Takenouti, H.; Torresi, R. *Electrochim. Acta* **1995**, *40*, 2755, 2765.
- (34) Gabrielli, C.; Keddám, M.; Minouflet, F.; Perrot, H. *Electrochim. Acta* **1996**, *41*, 1217.
- (35) Yang, H.; Kwak, J. *J. Phys. Chem. B* **1997**, *101*, 774.
- (36) Yang, H.; Kwak, J. *J. Phys. Chem. B* **1997**, *101*, 4656.
- (37) Yang, H.; Kwak, J. *J. Phys. Chem. B* **1998**, *102*, 1982.
- (38) Lee, H.; Yang, H.; Kim, Y. T.; Kwak, J. *J. Electrochem. Soc.* **2000**, *147*, 3801.
- (39) Gabrielli, C.; Keddám, M.; Nadi, N.; Perrot, H. *Electrochim. Acta* **1999**, *44*, 2095.
- (40) Gabrielli, C.; Keddám, M.; Nadi, N.; Perrot, H. *J. Electroanal. Chem.* **2000**, *485*, 101.
- (41) Gabrielli, C.; Keddám, M.; Perrot, H.; Pham, M. C.; Torresi, R. *Electrochim. Acta* **1999**, *44*, 4217.
- (42) Lang, G.; Inzelt, G. *Electrochim. Acta* **1999**, *44*, 2037.
- (43) Vorotyntsev, M. A.; Daikin, L. I.; Levi, M. D. *J. Electroanal. Chem.* **1994**, *364*, 37.
- (44) García-Jareño, J. J.; Sanmatias, A.; Vicente, F.; Gabrielli, C.; Keddám, M.; Perrot, H. *Electrochim. Acta* **2000**, *45*, 3765.
- (45) Gabrielli, C.; García-Jareño, J. J.; Perrot, H. *Hung. Electrochem.* **2000**, *137*, 269.
- (46) Buck, R. P. *J. Membr. Sci.* **1984**, *17*, 1.
- (47) Bruckenstein, S.; Hillman, A. R. *J. Phys. Chem.* **1988**, *92*, 4837.
- (48) Bruckenstein, S.; Hillman, A. R. *J. Phys. Chem.* **1991**, *95*, 10748.
- (49) Hillman, A. R.; Loveday, D. C.; Swann, M. J.; Bruckenstein, S.; Wilde, C. P. *J. Chem. Soc., Faraday Trans.* **1991**, *87*, 2047.
- (50) Siperko, L. M.; Kuwana, T. *J. Electrochem. Soc.* **1983**, *130*, 396.
- (51) Sauerbrey, G. *Z. Phys.* **1959**, *155*, 206.
- (52) García-Jareño, J. J.; Gabrielli, C.; Perrot, H. *Electrochem. Commun.* **2000**, *2*, 195.
- (53) García-Jareño, J. J.; Sanmatías, A.; Navarro-Laboulais, J.; Vicente, F. *Electrochim. Acta* **1998**, *44*, 395.
- (54) Zadronecki, M.; Wrona, P. K.; Galus, Z. *J. Electrochem. Soc.* **1999**, *146*, 620.
- (55) Gabrielli, C.; Takenouti, H.; Haas, O.; Tsukada, A. *J. Electroanal. Chem.* **1991**, *302*, 59.
- (56) Mathias, M. F.; Haas, O. *J. Phys. Chem.* **1992**, *96*, 3175.